HHS Public Access

Author manuscript

Cell Stem Cell. Author manuscript; available in PMC 2017 April 24.

Published in final edited form as:

Cell Stem Cell. 2016 October 06; 19(4): 530–543. doi:10.1016/j.stem.2016.07.004.

Proximity-based differential single cell analysis of the niche to identify stem/progenitor cell regulators

Lev Silberstein[1,2,3], **Kevin A Goncalves**[4,5], **Peter V Kharchenko**[2,6], **Raphael Turcotte**[2,7], **Youmna Kfoury**[1,2,3], **Francois Mercier**[1,2,3], **Ninib Baryawno**[1,2,3], **Nicolas Severe**[1,2,3], **Jacqueline Bachand**[1,2,3], **Joel Spencer**[1,2,3], **Ani Papazian**[1,2,3], **Dongjun Lee**[1,2,3], **Brahmananda Reddy Chitteti**[8], **Edward F Srour**[8], **Jonathan Hoggatt**[1,2,3], **Tiffany Tate**[1,2,3], **Cristina Lo Celso**[9], **Noriaki Ono**[10], **Stephen Nutt**[11], **Jyrki Heino**[12], **Kalle Sipilä**[12], **Toshihiro Shioda**[13], **Masatake Osawa**[14], **Charles P Lin**[2,7], **Guo-fu Hu**[4,5,*], and **David T Scadden**[1,2,3,*]

[1]Center for Regenerative Medicine, Massachusetts General Hospital, Boston, MA 02445, USA [2]Harvard Stem Cell Institute, Cambridge, MA 02138, USA [3]Department of Stem Cell and Regenerative Biology, Harvard University, Cambridge, MA 02138, USA [4]Graduate Program in Cellular and Molecular Physiology, Sackler School of Graduate Biomedical Sciences, Tufts University, Boston, MA 02111, USA [5]Molecular Oncology Research Institute, Tufts Medical Center, Boston, MA 02111, USA [6]Department for Biomedical Informatics, Harvard Medical School, Boston, MA 02115, USA [7]Wellman Center for Photomedicine, Massachusetts General Hospital, Boston, MA 02445, USA [8]Indiana University, Indianapolis, IN 46202, USA [9]Imperial College London, London SW7 2AZ, United Kingdom [10]University of Michigan School of Dentistry, Ann Arbor, MI 48109, USA [11]Walter and Eliza Hall Research Institute, Parkville Victoria 3052, Australia [12]University of Turku, Finland [13]Cancer Center, Massachusetts General Hospital, Boston, MA 02114, USA [14]Gifu University, Gifu, 501-1193, Japan

SUMMARY

Physiological stem cell function is regulated by secreted factors produced by niche cells. In this study, we describe an unbiased approach based on differential single-cell gene expression analysis of mesenchymal osteolineage cells close to and further removed from hematopoietic stem/progenitor cells to identify candidate niche factors. Mesenchymal cells displayed distinct molecular profiles based on their relative location. Amongst the genes which were preferentially expressed in proximal cells, we functionally examined three secreted or cell surface molecules not

[*]**Corresponding authors** Correspondence and requests for materials should be addressed to Guo-fu Hu (Guo-fu.Hu@tufts.edu) or David T Scadden (david_scadden@harvard.edu).

CONTRIBUTIONS

LS, MO and DTS conceived the project. LS, KAG, MO and DTS designed the experiments. LS, KAG, YK, FM, NO, NB, NS, JH, TT, AP, JB, EFS, BR, DL, JS, RT and TS performed the experiments. PVK performed bioinformatic analysis. LS, KAG, PVK, GFH, CLC and DTS analyzed the data. LS, KAG, PVK, GFH and DTS wrote the manuscript. SLN, GFH, JyH, KS provided reagents. We are grateful to David Clapham and Long-Jun Wu for technical advice, and to Jayaraj Rajagopal, Andrew Lane and Ya-Chieh Hsu for critical reading of the manuscript. We thank Charles Dinarello for technical advice, Laura Prickett, Kathryn Folz-Donahue and Meredith Weglarz for cell sorting and Edward Fox at Dana Farber Cancer Institute Microarray core for cDNA sequencing.

COMPETING FINANCIAL INTERESTS

David T Scadden is a shareholder in Fate Therapeutics and a consultant for Fate Therapeutics, Hospira, GSK, and Bone Therapeutics. Drs Silberstein, Kharchenko, Hu, Goncalves and Scadden filed patent applications related to the findings described in the manuscript. The remaining authors declare no competing financial interests.

previously connected to HSPC biology: the secreted RNase Angiogenin, the cytokine IL18 and the adhesion molecule Embigin and discovered that all of these factors are HSPC quiescence regulators. Our proximity-based differential single cell approach therefore reveals molecular heterogeneity within niche cells and can be used to identify novel extrinsic stem/progenitor cell regulators. Similar approaches could also be applied to other stem cell/niche pairs to advance understanding of microenvironmental regulation of stem cell function.

Keywords

stem cell niche; single cell analysis; hematopoiesis

INTRODUCTION

Inter-cellular communications are essential for maintenance of tissue homeostasis and response to injury, as exemplified by functional relationship between stem/progenitor cells and their microenvironment, or niche. Studies first experimentally validating the niche concept leveraged proximity of heterologous cells (Xie and Spradling, 2000). Subsequent studies in multiple species and tissues have convincingly demonstrated that the niche serves as a critical regulatory unit to ensure preservation and optimal functioning of the stem cell pool (Moore and Lemischka, 2006) (Hsu et al., 2014) (Chakkalakal et al., 2012) (Li and Clevers, 2010) (Byrd and Kimble, 2009) (Fuentealba et al., 2012).

Hematopoietic stem cell and progenitor cell (HSPC) bone marrow niche has been extensively studied (Mendelson and Frenette, 2014) using cell ablation or cell type-specific gene deletion experiments (Morrison and Scadden, 2014). Niche participants have been defined as including endothelial cells, multiple mesenchymal types: adipocytes, CXCL12+ adventitial reticular (CAR) cells, osteolineage cells (OLC), LeptinR+ and nestin+ cells, NG2+ arteriolar sheath cells; non-myelinated Schwann cells and hematopoietic cells: macrophages and megakaryocytes (Mendelson and Frenette, 2014). The molecular regulators defined, however, are limited and most recent studies have focused on CXCL12 and stem cell factor (Ding and Morrison, 2013; Ding et al., 2012; Greenbaum et al., 2013). We sought to seek novel regulators by reverting back to basic principles of niches, that cells in close proximity form an interactive physiologic unit. To experimentally exploit that principle, we used the microanatomy of HSPC in bone marrow to guide single cell sampling and analysis.

We focused on the post-transplant bone marrow niche because of its direct relevance to the clinical setting of HSPC recovery following transplantation. We emphasize that the post-transplant niche critically differs from the homeostatic niche in two major aspects. First, the niche functions to support HSPC during regeneration and expansion as opposed to steady state when most HSPCs remain dormant. Second, the molecular and cellular composition of the post-transplant niche is markedly distinct due to the toxic effect of irradiation conditioning on the niche constituents. In particular, perivascular and endothelial cells, known to serve as a major source of critical niche factors such as CXCL12 and stem cell factor, are destroyed (Zhou et al, 2015) while the osteolineage cells (OLCs), also shown to

play a regulatory role in HSPC niche (Calvi et al., 2003; Sugimura et al., 2012; Zhang et al., 2003), not only survive irradiation but transiently expand (Dominici et al., 2009) thus making it feasible to study these cells in the post-transplant setting.

Prior *in vivo* imaging studies of the post-transplant niche by our group and others demonstrated that in irradiated animals, some transplanted HSPC are found in close proximity to the endosteal surface and OLCs labeled by col2.3GFP transgene (Lo Celso et al., 2009; Xie et al., 2009), as defined by their location within two cell diameters from individual OLC. Given that spatial proximity between niche cells and primitive cells governs functional organization of stem cell niches from nematodes to mammals (Moore and Lemischka, 2006), we reasoned that HSPC-OLC co-localization in the post-transplant bone marrow niche may be similarly indicative of a regulatory relationship. If this is the case, it implies that OLCs may be heterogeneous: those which are located in close proximity to single transplanted HSPC ("proximal OLCs") are most intimately involved in HSPC control while those at the distance ("distal OLCs") are less likely to be engaged in the niche-related function. Therefore, proximal OLC signature, as defined by transcriptional comparison to the distal OLC cell subset, could serve as a valuable resource for unbiased identification of HSPC regulatory molecules in vivo.

RESULTS

Experimental platform for proximity-based study of HSPC niche

In order to undertake proximity-based analysis of post-transplant bone marrow niche, we adapted the same experimental platform as used in the above-mentioned in vivo imaging studies (Lo Celso et al., 2009) except for performing the experiments in neonatal col2.3GFP + recipients, which offered access to fresh bone tissue without decalcification.

Histological examination of bone sections from newborn animals transplanted with adult bone marrow LT-HSCs (lineage-negative (lin-) kit^+ $Sca1^+$ [LKS] $CD34^-Flk2^-$) fluorescently labeled with a lipophilic membrane-bound dye, DiI, demonstrated that at 48 hours, some single DiI-labeled cells were found in close proximity to individual OLCs (Figure 1A). For the subsequent experiments, proximal OLC was defined as the nearest cell within two cell diameters from a single DiI+ cell, while distal OLCs were harvested from the remaining OLC pool based on their location *at least* five HSPC cell diameters away from transplanted cells (Figure 1A). We also observed some transplanted DiI+ cells forming clusters, but these were usually located away from the OLC-covered endosteal surface and were not part of a definition of either proximal or distal OLCs (Figure S1).

Following transplantation, we extracted individual proximal and distal OLCs from fresh sections of femoral bones, performed single cell RNA-Seq analysis and validated differentially expressed genes as niche-derived HSPC regulators in vivo (Figure 1B). In order to retrieve OLCs directly from a section of neonatal trabecular bone, we modified the standard patch clamp microscopy platform by introducing additional steps for tissue immobilization and *in situ* enzymatic digestion under direct visual control followed by micropipette aspiration (Figure 1C).

Proximal OLCs have a distinct transcriptional signature

In total, sixteen proximal OLCs and sixteen distal OLCs were retrieved. Following quality control assessment of single cell cDNA amplification [see Methods], eight cells from each group were selected for single cell RNA-Seq analysis.

To test whether proximal and distal OLCs could be distinguished in an unbiased manner based on a genome-wide transcriptional signature, we performed cross-validation tests using the "leave-two-out" strategy. Specifically, transcriptional signatures of one proximal and one distal OLC were "left out" from the dataset, a machine-learning classifier was trained on the remaining cells, and the ability of the classifier to correctly assign the transcriptomes of the "left-out" cells to either proximal or distal group was evaluated (Rizzo, 2007). The process was repeated for all proximal-distal cell pairs (64 possible combinations in total). Despite a small sample size, the majority of "left-out" samples were correctly classified (Figure 2A, area under the curve AUC=0.854, $p<10^{-5}$) indicating that the proximal and distal OLCs displayed stable genome-wide transcriptional differences and that the molecular signature was reliable even though derived from a modest number of cells.

Single-cell RNA-Seq data exhibits higher levels of technical noise than the bulk measurements, as was also the case with our samples. In order to accommodate for biological and technical noise and improve the resolution of expression differences at the level of individual genes, we developed a probabilistic method, which uses Bayesian approach to estimate the likelihood of expression magnitude based on the observed reads for a gene in question and the overall error characteristics within the transcriptome of a particular single cell sample – Single Cell Differential Expression (SCDE)(Kharchenko et al., 2014). By evaluating posterior probability of expression magnitude for a given gene in each cell, the method is able to assess the overall likelihood that expression of a gene differs between proximal and distal OLCs (Vcam-1 gene shown as a representative example, Figure 2B, the list of top differentially expressed genes in Table 1). The complete proximal/distal OLC database can be accessed via the URL http://pklab.med.harvard.edu/sde/viewpost.html?dataset=olc

Using the top 200 differentially expressed genes, we found that profiles of proximal OLCs are clustered separately from the profiles of distal OLCs (Figure 2C). In particular, gene set enrichment analysis showed that proximal OLCs displayed a significant up-regulation of genes encoding cell surface proteins (p-value 6.8×10^{-4}, Q-value 0.048; top genes: Vcam1, Adam9, Amot) and those involved in immune response (p-value 3.1×10^{-6}, Q-value 0.0090; top genes: Map3k14, Cxcl12, Il18), supporting their role in intercellular communications (Figure S2). At the level of individual genes, we found that with the exception of c-kit, proximal OLCs had significantly higher expression levels of niche-associated molecules (most notably Cxcl12 and Vcam-1) as compared to distal OLCs. Further, in accordance with prior studies of a regulatory OLC phenotype, proximal OLCs were lineage-committed ($Runx2^{+}$, $Sp7/osterix^{+}$, $col1a1^{+}$) but less mature ($Spp1/osteopontin^{low}$, $Bglap/osteocalcin^{low}$, $Dmp1^{low}$) than distal OLCs (Figure 2D,E). To emphasize, the proximal OLC were immature cells of osteolineage, not mature osteoblasts.

To verify whether proximity-associated OLC heterogeneity revealed by single cell RNA-Seq experiments can be also demonstrated within the tissue, we performed fluorescent *in situ* hybridization experiments (RNA Scope), a recently developed method that allows for quantitative measures of gene expression (Wang et al., 2012). We focused on one of the factors that we also tested for function *in vivo*, interleukin 18 (IL18). Bone sections from newborn col2.3GFP+ animals 48 hours after transplantation with DiI-labeled LT-HSC (the identical experimental setting as for cell-harvesting) were examined. We focused on IL 18 expression in GFP-labeled OLCs, although the IL18 signal was not restricted to these cells, as previously reported (Novick et al., 2013). We defined "proximal" (within two cell diameters) and distal (greater than five cell diameters) areas as shown and quantified the amount of target RNA molecules as a number of dots per GFP+ cell (Figure 2F). We found that GFP+ OLCs in the proximal area contain a higher number of IL18 transcripts per cell as compared to those located further away ($P<2.2\times10^{-4}$).

Taken together, these data demonstrate that micro-anatomical proximity to a heterologous cell acts as a powerful and reliable discriminator between molecularly distinct subset within an apparently homogeneous, lineage-restricted cell population and identifies a subset of immature OLCs whose signature is consistent with an HSPC regulatory function.

In light of these findings, we set out to test whether the proximal OLC signature could be used as a resource for identification of novel non cell-autonomous HSPC regulators *in vivo*. Based on availability of *in vivo* models for functional testing, we chose three membrane-bound and secreted factors for further validation: secreted RNase angiogenin (ANG), pro-inflammatory cytokine interleukin 18 (IL18), and cell adhesion molecule Embigin.

ANG regulates LT-HSC quiescence and self-renewal

ANG is a secreted ribonuclease with established roles in promoting tumor angiogenesis and cellular proliferation (Kishimoto et al., 2005). It also acts as a neuronal pro-survival factor in amyotrophic lateral sclerosis (ALS) (Greenway et al., 2006).

We found that *Ang* was expressed at a higher level in proximal OLCs (Figure 3A) and undertook a functional evaluation of its role in the bone marrow niche by conditionally deleting *Ang* from distinct niche cell subsets. We crossed *Ang* "floxed" mice with animals in which tamoxifen-inducible *Cre*-recombinase was driven by the promoters targeting specific mesenchymal cells – osteolineage committed progenitors (*Osx*) (Mizoguchi et al., 2014), mesenchymal progenitors (*nestin*) (Mendez-Ferrer et al., 2010), periarteriolar sheath cells (*NG2*) (Zhu et al., 2011) and mature osteoblasts (*Col1a1*) (Kim et al., 2004). *Ang* expression in these niche cell subsets has been previously documented (Kunisaki et al., 2013) (Paic et al., 2009).

All conditional knock-outs demonstrated no significant changes in peripheral blood or bone marrow, apart from mild lymphocytosis (Table 2). However, immunophenotypic analysis of primitive hematopoietic cells (Figure S3A) revealed that deletion of *Ang* from Osx^+, Nes^+ and $NG2^+$ cells resulted in an increase of the number of LT-HSC and more active cycling of LT-HSC, short-term HSC (ST-HSC) and multi-potent progenitors (MPP) (Figure 3B,C and Figure S3Bi,ii, C, Di,ii). In contrast, *Ang* deletion in mature osteoblasts by *col1a1*Cre had no

effect on these cell populations, but was associated with an increase in number and more active cycling of common lymphoid progenitors (CLP), as was also seen upon *Ang* deletion from Nes^{+} and $NG2^{+}$ cells (Figure 3D,E). The number and cell cycle status of the myeloid progenitors in any of the above strains were unaffected by the *Ang* deletion (Figure S3 Biii, Diii).

To assess the effect of the above-noted changes on long-term hematopoietic reconstitution, we competitively transplanted the bone marrow from $Ang^{fl/fl}$OsxCre, $Ang^{fl/fl}$NesCre, $Ang^{fl/fl}$NG2Cre, and $Ang^{fl/fl}$Col1a1Cre mice and corresponding controls into congenic WT recipients (Figure 3F). We observed significantly reduced long-term multi-lineage reconstitution in the recipients of the bone marrow from $Ang^{fl/fl}$OsxCre osteoolineage progenitors, $Ang^{fl/fl}$NesCre, $Ang^{fl/fl}$NG2Cre mice while the animals which were transplanted with $Ang^{fl/fl}$Col1a1Cre mature osteoblast bone marrow displayed only a lymphoid reconstitution defect. Taken together, our observations reveal the role of ANG as a niche-derived regulator of quiescence and long-term reconstitution LT-HSC, ST-HSC, MPP and CLP and highlight differences in the target cell populations depending on a cellular source: ANG produced by mesenchymal progenitors, osteolineage committed progenitors and peri-arteriolar sheath cells regulates quiescence and repopulating ability of LT-HSC, while ANG derived from mature osteoblasts regulates lymphoid progenitors. Our findings that the absence of ANG in the microenvironment results in a long-term reconstitution defect raised a possibility that exposure to recombinant ANG may activate HSPC self-renewal program under the conditions of proliferative stress. This hypothesis was tested in a follow-up study by us (Goncalves et al, accepted in *Cell*), which showed that ex-vivo treatment of LT-HSC with recombinant ANG prior to transplant or in vivo administration post-irradiation significantly enhances the regenerative capacity of HSPC.

IL 18 regulates quiescence of short-term hematopoietic progenitors

IL18 is a component of inflammasome, which is expressed by multiple cell types within and outside the bone marrow and stimulates interferon-gamma production by T-cells (Okamura et al., 1995), but has no known regulatory effect on HSPCs. We tested it in that setting given that our proximity-based analysis revealed IL18 expression in proximal OLCs: none of the distal OLCs had detectable IL18 transcripts (Figure 4A).

Notably, we found IL18R1 on the cell surface of short-term progenitors, but not LT-HSC (Figure 4B). To determine a functional role for IL18, we evaluated IL18 knock-out (IL18KO) mice and while no abnormalities in mature cell number were noted in the bone marrow and in peripheral blood at baseline (apart from modest neutrophilia) (Figure S4 A-C), cell cycle and BrdU incorporation studies revealed increased proliferative rate in short-term hematopoietic progenitors - ST-HSC and MPP - but not in LT-HSC (Figure 4C and Figure S4D). These observations are consistent with IL18 regulating the quiescence of short-term progenitors.

Because IL18 is a stress-response molecule, we wondered if its effect on HSPC would be greater in the setting of recovery from bone marrow injury, such as exposure to the cell cycle-specific genotoxin 5-fluorouracil (5-FU). Quantification of progenitor cell subsets 7 days post-exposure to 5-FU (Broxmeyer et al., 2012) showed a significantly increased

frequency of LKS cells, lin^{-} $kit^{+}Sca1^{-}$ myeloid progenitors and CLPs in IL18KO mice, as compared to 5-FU-treated WT controls (Figure 4D). In newborn IL18KO animals, loss of HSPC quiescence at baseline and exaggerated response to genotoxic injury (busulphan exposure in utero) (Bruscia et al., 2006) were also observed (Figure S5E). Taken together, these data suggest that IL18 constrains progenitor proliferation.

To further evaluate this function, we treated animals with recombinant IL18 and found that it protected LKS cells from 5-FU-induced apoptosis (Figure 4E) but limited the vigor of marrow recovery, as evidenced by decreased frequency of lineage-negative cells (Figure 4E). The specificity of these findings was confirmed by performing an identical experiment in IL18R1KO mice, which were unresponsive to exogenously administered IL18 (Figure S4F). Therefore, IL18 can protect progenitors from cell cycle specific genotoxins, but in so doing suppresses progenitor response to injury, restraining hematopoietic recovery.

To test if the quiescence-inducing effect of IL18 on short-term progenitors is exerted in a non cell-autonomous fashion, we transplanted WT (CD45.1) bone marrow cells into lethally irradiated IL18KO or WT recipients (CD45.2). We found that the IL18-deficient environment in the recipient animals conferred a significantly faster short-term hematopoietic recovery without affecting long-term reconstitution in both primary and secondary transplants (Figure S5A). In keeping with this, transplantation of the progenitor-enriched WT bone marrow fraction (LKS cells) into IL18KO hosts was accompanied by approximately 2-fold increase in both myeloid (week 2) and lymphoid (week 4) cells in peripheral blood of the recipient animals (Figure 4F). The finding of enhanced early post-transplant reconstitution in the absence of IL18 signaling was recapitulated in a reciprocal experiment, when sorted LKS cells from IL18 receptor knock-out animals were transplanted into WT hosts (Figure 4G), indicating that the effect of IL18 on short-term progenitors is likely to be direct. In both sets of experiments, enhanced reconstitution was multi-lineage but did not persist long-term, consistent with the predominant effect of IL18 on multi-potent short-term progenitors (Figure S5B,C). Interestingly, faster proliferation of transplanted LKS cells in IL18KO recipients was already evident at 24 hours, as shown by intra-vital imaging studies, and was associated with homing further away from the endosteal surface indicating that IL18 also regulates progenitor localization in the niche (Figure S5D).

To test if the effect of IL18 on post-transplant progenitor expansion can be exploited therapeutically, we transplanted lethally irradiated IL18KO and WT recipients with a limiting dose of WT bone marrow and found improved survival in the IL18KO group (Figure S5E). Given that IL18R is expressed in human HSPC (Fig. S5F), our results create a rationale for further translational studies to test whether that IL18 neutralization might be a means of reducing post-transplant cytopenias – a major cause of morbidity and mortality in patients.

Embigin regulates HSPC localization and quiescence and defines niche-factor enriched OLC subset

Embigin is a cell adhesion molecule of immunoglobulin superfamily (Huang et al., 1990, 1993). Embigin is thought to enhance integrin-dependent cell substrate adhesion and was also shown to promote neuromuscular synapse formation (Lain et al., 2009). Embigin is

widely expressed within the hematopoietic system, including primitive hematopoietic cells (Pridans et al., 2008), but its function remains obscure.

Our proximity-based analysis showed that proximal OLCs had a significantly higher level of Embigin expression compared to distal OLCs (Figure 5A), and we undertook *in vivo* functional studies to evaluate its role as a hematopoietic regulator using anti-Embigin monoclonal antibody (Pridans et al., 2008).

We found that injection of WT animals with anti-Embigin is associated with approximately 2-fold increase in the frequency of LT-HSCs, ST-HSCs, MPP and colony-forming cells as compared to those treated with isotype control antibody (Figure 5B,C). Further, there was a reduction in the proportion of cells in G0 phase of the cell cycle (Figure 5D) with a corresponding increase in S/G2/M phase and increased BrdU incorporation by primitive hematopoietic cells (Figure S6A), overall indicating the loss of HSPC quiescence upon anti-Embigin treatment.

Given that Embigin is a cell adhesion molecule, we tested the effect of anti-Embigin on HSPC localization. We found that injection of anti-Embigin resulted in mobilization of lineage–negative kit+ progenitors and colony-forming cells (CFC), but not LKS cells, into the blood (Figure 5E). On the other hand, intra-vital microscopy studies revealed that either *in vitro* incubation of LKS cells [known to express Embigin] (Forsberg et al., 2010) with anti-Embigin or injection of anti-Embigin into lethally irradiated hosts resulted in a significantly lower number of transplanted LKS cells reaching calvarial bone marrow as compared to an isotype control (Figure 5F,G, left panels, Figure S6B,C), thus consistent with Embigin functioning as a homing molecule.

Notably, we observed that WT LKS cells transplanted into anti-Embigin pre-treated recipients or those pre-treated with anti-Embigin antibody displayed a higher proliferation rate (Figure 5F,G, right panels), measured as a ratio of cell number per calvarial bone marrow between 48 hours and 24 hours post-transplant. We verified the imaging data on homing and proliferation data by flow cytometric assessment of frequency and cell cycle status of transplanted cells (Figure S6 D,E). These results demonstrated that the effect of anti-Embigin on HSPC is direct and not primarily driven by depletion of mature leucocytes which was previously reported following anti-Embigin administration (Pridans et al., 2008). Consistent with the effect of anti-Embigin on HSPC quiescence and homing, bone marrow from anti-Embigin treated animals reconstituted poorly when competitively transplanted into irradiated recipients as compared to isotype-control treated marrow (Figure S6F). A quiescence-inducing effect of Embigin was further confirmed by intra-vital imaging experiments using Embigin KO mice which were made available in a limited number through collaboration: irradiated WT and Embigin KO animals were transplanted with WT LKS cells fluorescently labeled wit DiI, and the number of DiI+ singlets and clusters in the calvarial bone marrow were quantified 24 hours post-injection. We observed a significantly higher cluster/singlet ratio in Embigin KO recipients, indicative of greater proliferation in the absence of niche-derived Embigin (Figure S6G). No homing defect was detectable suggesting that the effects of anti-Embigin antibody on HSPC localization may be due to

acute Embigin blockade (as opposed to constitutive absence) or downstream signaling upon antibody binding which need to be further investigated.

Taken together, our results with are consistent with Embigin function as a regulator of HSPC localization and quiescence and provide the rationale for future mechanistic studies to examine the role of Embigin in HSPC regeneration.

In addition to identifying the functional role of Embigin in the niche, we asked if Embigin can be used as a cell surface marker for prospective isolation of a niche factor-enriched OLC subset. We therefore performed flow cytometric analysis of single cell suspensions isolated from bones of adult col2.3GFP mice using antibodies against Embigin in combination with VCAM1-another cell surface molecule which was preferentially expressed in proximal OLCs and easily detectable with commercially available antibody. These experiments revealed the presence of a distinct Embigin ^{high} VCAM1^{+}population which we termed “VE cells” (for VCAM and Embigin)(Figure 6A). Transcriptome comparison of VE and non-VE (remaining col2.3GFP+ OLCs) cells demonstrated that VE cells are immature and enriched for known HSPC niche factors, thus resembling proximal OLCs (Figure 6B). VE cells had a distinct transcriptional profile compared to other niche populations such as nestin-GFP^{high} and nestin-GFP^{low} cells, as revealed by PCA analysis (Figure 6C). Since the proximal OLC analysis had defined an immunophenotypic method of prospectively isolating similar cells, we reasoned that we could now perform flow based isolation and characterization of the VE subset under different conditions.

Testing this strategy, we first exposed animals to lethal irradiation to assess the impact of conditioning on a specific niche subset. Notably, VE cells increased in frequency and displayed up-regulation of two major HSPC retention molecules, CXCL12 and VCAM1, while the expression of these molecules in non-VE cells remained unchanged (Figure 6D,E). We also then asked whether niche cells ‘see’ and respond to the hematopoietic cells they support by examining VE cell gene expression after infusion of either cells or saline post-irradiation conditioning. Intriguingly, VE cells differentially changed their gene expression when LT-HSCs versus saline were injected into lethally irradiated col2.3GFP+ mice. Specifically a cell-cell adhesion gene set, as determined by gene set enrichment analysis (GSEA), was upregulated (P-value 7.8×10^{-5}, Q-value 0.019, top genes Nrcam, Icam2, Esam) whereas non-VE cells did not display consistent changes in this or other GSEA pathways tested (Figure 6F and data not shown). Thus, using Embigin as a cell surface marker defined a subset of immature OLCs which is enriched in niche factors and displays differential responsiveness to local and environmental cues. These data indicate that hematopoietic cells regulate their niche: a concept complementing the well-defined notion that the niche regulates hematopoietic cells.

DISCUSSION

These studies illustrate several methodological and biological principles. First, we show that while single cell analysis has frequently been used to define heterogeneity among admixed cells, applied to reveal differential gene expression between cells of specific micro-anatomic position can be uniquely powerful in identifying cell subsets and molecules of functional

importance. We demonstrate that utilizing the key principle of niche organization – mesenchymal-parenchymal proximity – as an upfront biological filter one can define otherwise indistinguishable stromal mesenchymal cell subsets. Given that proximity between a niche cell and a stem/progenitor cell is a common feature of normal and malignant niches, we believe that our approach - possibly in conjunction with other in-situ transcriptome analysis platforms such as MER FISH (Chen et al., 2015), FISSEQ (Lee et al., 2014) or TEVA (Lovatt et al., 2014) – can be more generally applied in other tissue contexts.

Second, we show that combining proximity and single cell analysis can define novel factors that regulate neighboring cells. Our approach to regulatory factor identification was unbiased since we had no the prior knowledge of the cells which we interrogated (proximal OCLs) and the molecules which they produce as being involved in HSPC regulation. We focused on signaling molecules that were on the cell surface or secreted and could therefore act in a paracrine manner without necessitating direct cell-cell contact, and performed our experiments in the setting of transplantation because of our interest in defining molecular regulators that may be of relevance to medicine. All three niche factors demonstrated potential value in animal models relevant to clinical settings such as sensitivity to chemotherapy, recovery from genotoxic insult or hematopoietic regeneration following myeloablative transplantation. Perhaps most promisingly from a translational standpoint, our follow-up studies (Goncalves et al, accepted in *Cell*) revealed that ex-vivo exposure of mouse or human HSPC to recombinant Angiogenin or systemic administration of ANG post-irradiation in mice significantly boosts hematopoietic reconstitution. Thus, our discovery platform led to development of novel approaches to enhance hematopoietic regeneration in clinic.

Third, we demonstrate that our approach can reveal a subset of proximal-like cells (VE cells) that can be subsequently isolated by flow cytometry and molecularly analyzed. Doing so in the context of hematopoietic stem cell transplantation, we demonstrate that VE cells display a different pattern of gene expression in the presence of transplanted HSPC. These data indicate that niche cells are affected by the presence of the stem/progenitor cells they support. Therefore, there is bi-directional communication between specific niche stromal cells and stem/progenitor cells in the bone marrow. Similar, reciprocally modulating functional units may exist in other tissue niches.

It was striking that the three molecules we identified by differential single cell gene expression all regulate HSPC quiescence, despite the molecules representing very distinct functional classes (a secreted RNAase, a cytokine and an adhesion regulator). This may be coincidence, but it does pose the question of whether there are niches in the marrow microenvironment that are particularly abundant in quiescence-inducing or activation-inducing molecules and may therefore serve as function-specific niches.

In summary, we show that reverting to the basic principle of niches that heterologous cells in proximity can regulate each other and combining that with differential single cell analysis can be a powerful means of identifying new biologically relevant molecular regulators and defining concepts like reciprocal interaction. Our proximity-based differential single cell

analysis platform can serve as a discovery approach to identify new molecular and cellular aspects of niche biology.

METHODS

For the details of animal models, data analysis, flow cytometry, transplantation, 5-FU treatment, BrdU incorporation, mobilization experiments and gene expression studies please see Extended Experimental Procedures.

Single OLC harvesting and single cell RNA-Seq

Newborn col2.3GFP animals were injected with DiI- labeled LKS CD34^{-}Flk2^{-} adult bone marrow cells and sacrificed 48 hours after transplantation. Femurs were dissected, embedded in 10% low melting temperature agarose (Lonza) and sectioned at 100μ using a vibratome (Leica). Single OLC harvesting was performed using a physiology microscope BX51 (Olympus) equipped with filters to detect GFP and DiI fluorescence, DIC optics, micromanipulators (Eppendorff), real-time imaging camera, peristaltic pump, in-line heater, perfusion chamber (Harvard Apparatus) and SAS Air Syringe (Research Instruments). Sections were pre-screened for the presence of rare GFP-labeled OLCs located next to single DiI-positive transplanted HSCPs, which were found in 1-2 out of 15 sections per animal. The section was secured against the bottom of the perfusion chamber with holding pipette (Humagen) and was perfused with warm (37°C) cell dissociation solution (Liberase TM, Roche) for 8-10 minutes while the target cell was visually monitored. Then, applying positive pressure from the micropipette using Air Syringe, hematopoietic cells surrounding the target OLC were dislodged to create a 20-30 μ clearing. Finally, the aspiration pipette was lowered onto the target OLC, the cell was gently detached from the endosteal surface and aspirated. The presence of GFP fluorescence in the aspirated cell inside the aspiration pipette was confirmed, and the contents of the pipette was ejected into a PCR tube with the lysis buffer for the single cell RNA-Seq (Tang et al., 2009) and frozen immediately at −80°C.

Bioinformatics and single cell RNA-Seq data analysis

The differential expression estimates were obtained from single-cell RNA-seq data using the approach described in Supplementary Experimental Procedures. The single cell and bulk analysis RNA-Seq data has been deposited in GEO under accession number GSE52359. The full differential expression analysis can be viewed via the following URL http://pklab.med.harvard.edu/sde/viewpost.html?dataset=olc

Supplementary Material

Refer to Web version on PubMed Central for supplementary material.

Acknowledgments

FUNDING

The work was supported by fellowship awards from Leukemia and Lymphoma Research UK and Leukemia and Lymphoma Society (LS), T32 Training Fellowship (JH), NIH grants K25AG037596 (PVK), R01DK050234 and

R01HL097794(DTS), R01CA105241 and R01NS065237 (GFH), NIH F31HL128127 (KAG), Sackler Dean's Fellow Award (KAG), Sackler Families Collaborative Cancer Biology Award (KAG/GFH), National Health and Medical Research Council of Australia Fellowship (SLN), the Victorian State Government Operational Infrastructure Support (SLN) and Australian Government NHMRC IRIIS (SLN).

References

Adams GB, Martin RP, Alley IR, Chabner KT, Cohen KS, Calvi LM, Kronenberg HM, Scadden DT. Therapeutic targeting of a stem cell niche. Nat Biotechnol. 2007; 25:238–243. [PubMed: 17237769]

Arora N, Wenzel PL, McKinney-Freeman SL, Ross SJ, Kim PG, Chou SS, Yoshimoto M, Yoder MC, Daley GQ. Effect of developmental stage of HSC and recipient on transplant outcomes. Developmental cell. 2014; 29:621–628. [PubMed: 24914562]

Broxmeyer HE, Hoggatt J, O'Leary HA, Mantel C, Chitteti BR, Cooper S, Messina-Graham S, Hangoc G, Farag S, Rohrabaugh SL, et al. Dipeptidylpeptidase 4 negatively regulates colony-stimulating factor activity and stress hematopoiesis. Nature medicine. 2012; 18:1786–1796.

Bruscia EM, Ziegler EC, Price JE, Weiner S, Egan ME, Krause DS. Engraftment of donor-derived epithelial cells in multiple organs following bone marrow transplantation into newborn mice. Stem cells. 2006; 24:2299–2308. [PubMed: 16794262]

Byrd DT, Kimble J. Scratching the niche that controls Caenorhabditis elegans germline stem cells. Seminars in cell & developmental biology. 2009; 20:1107–1113. [PubMed: 19765664]

Calvi LM, Adams GB, Weibrecht KW, Weber JM, Olson DP, Knight MC, Martin RP, Schipani E, Divieti P, Bringhurst FR, et al. Osteoblastic cells regulate the haematopoietic stem cell niche. Nature. 2003; 425:841–846. [PubMed: 14574413]

Chakkalakal JV, Jones KM, Basson MA, Brack AS. The aged niche disrupts muscle stem cell quiescence. Nature. 2012; 490:355–360. [PubMed: 23023126]

Chen KH, Boettiger AN, Moffitt JR, Wang S, Zhuang X. RNA imaging. Spatially resolved, highly multiplexed RNA profiling in single cells. Science. 2015; 348:aaa6090. [PubMed: 25858977]

Ding L, Morrison SJ. Haematopoietic stem cells and early lymphoid progenitors occupy distinct bone marrow niches. Nature. 2013; 495:231–235. [PubMed: 23434755]

Ding L, Saunders TL, Enikolopov G, Morrison SJ. Endothelial and perivascular cells maintain haematopoietic stem cells. Nature. 2012; 481:457–462. [PubMed: 22281595]

Dominici M, Rasini V, Bussolari R, Chen X, Hofmann TJ, Spano C, Bernabei D, Veronesi E, Bertoni F, Paolucci P, et al. Restoration and reversible expansion of the osteoblastic hematopoietic stem cell niche after marrow radioablation. Blood. 2009; 114:2333–2343. [PubMed: 19433859]

Forsberg EC, Passegue E, Prohaska SS, Wagers AJ, Koeva M, Stuart JM, Weissman IL. Molecular signatures of quiescent, mobilized and leukemia-initiating hematopoietic stem cells. PloS one. 2010; 5:e8785. [PubMed: 20098702]

Fuentealba LC, Obernier K, Alvarez-Buylla A. Adult neural stem cells bridge their niche. Cell Stem Cell. 2012; 10:698–708. [PubMed: 22704510]

Greenbaum A, Hsu YM, Day RB, Schuettpelz LG, Christopher MJ, Borgerding JN, Nagasawa T, Link DC. CXCL12 in early mesenchymal progenitors is required for haematopoietic stem-cell maintenance. Nature. 2013; 495:227–230. [PubMed: 23434756]

Greenway MJ, Andersen PM, Russ C, Ennis S, Cashman S, Donaghy C, Patterson V, Swingler R, Kieran D, Prehn J, et al. ANG mutations segregate with familial and 'sporadic' amyotrophic lateral sclerosis. Nature genetics. 2006; 38:411–413. [PubMed: 16501576]

Hoggatt J, Mohammad KS, Singh P, Hoggatt AF, Chitteti BR, Speth JM, Hu P, Poteat BA, Stilger KN, Ferraro F, et al. Differential stem- and progenitor-cell trafficking by prostaglandin E2. Nature. 2013; 495:365–369. [PubMed: 23485965]

Hsu YC, Li L, Fuchs E. Emerging interactions between skin stem cells and their niches. Nature medicine. 2014; 20:847–856.

Huang RP, Ozawa M, Kadomatsu K, Muramatsu T. Developmentally regulated expression of embigin, a member of the immunoglobulin superfamily found in embryonal carcinoma cells. Differentiation. 1990; 45:76–83. [PubMed: 1965893]

Huang RP, Ozawa M, Kadomatsu K, Muramatsu T. Embigin, a member of the immunoglobulin superfamily expressed in embryonic cells, enhances cell-substratum adhesion. Dev Biol. 1993; 155:307–314. [PubMed: 8432389]

Johnson WE, Li C, Rabinovic A. Adjusting batch effects in microarray expression data using empirical Bayes methods. Biostatistics. 2007; 8:118–127. [PubMed: 16632515]

Kalajzic I, Kalajzic Z, Hurley MM, Lichtler AC, Rowe DW. Stage specific inhibition of osteoblast lineage differentiation by FGF2 and noggin. Journal of cellular biochemistry. 2003; 88:1168–1176. [PubMed: 12647299]

Kharchenko P, Silberstein L, Scadden DT. Bayseian approach to single cell differential expression analysis. Nature Methods. 2014

Kim JE, Nakashima K, de Crombrugghe B. Transgenic mice expressing a ligand- inducible cre recombinase in osteoblasts and odontoblasts: a new tool to examine physiology and disease of postnatal bone and tooth. The American journal of pathology. 2004; 165:1875–1882. [PubMed: 15579432]

Kishimoto K, Liu S, Tsuji T, Olson KA, Hu GF. Endogenous angiogenin in endothelial cells is a general requirement for cell proliferation and angiogenesis. Oncogene. 2005; 24:445–456. [PubMed: 15558023]

Kunisaki Y, Bruns I, Scheiermann C, Ahmed J, Pinho S, Zhang D, Mizoguchi T, Wei Q, Lucas D, Ito K, et al. Arteriolar niches maintain haematopoietic stem cell quiescence. Nature. 2013; 502:637–643. [PubMed: 24107994]

Lain E, Carnejac S, Escher P, Wilson MC, Lomo T, Gajendran N, Brenner HR. A novel role for embigin to promote sprouting of motor nerve terminals at the neuromuscular junction. The Journal of biological chemistry. 2009; 284:8930–8939. [PubMed: 19164284]

Lee JH, Daugharthy ER, Scheiman J, Kalhor R, Yang JL, Ferrante TC, Terry R, Jeanty SS, Li C, Amamoto R, et al. Highly multiplexed subcellular RNA sequencing in situ. Science. 2014; 343:1360–1363. [PubMed: 24578530]

Li L, Clevers H. Coexistence of quiescent and active adult stem cells in mammals. Science. 2010; 327:542–545. [PubMed: 20110496]

Lo Celso C, Fleming HE, Wu JW, Zhao CX, Miake-Lye S, Fujisaki J, Cote D, Rowe DW, Lin CP, Scadden DT. Live-animal tracking of individual haematopoietic stem/progenitor cells in their niche. Nature. 2009; 457:92–96. [PubMed: 19052546]

Lovatt D, Ruble BK, Lee J, Dueck H, Kim TK, Fisher S, Francis C, Spaethling JM, Wolf JA, Grady MS, et al. Transcriptome in vivo analysis (TIVA) of spatially defined single cells in live tissue. Nat Methods. 2014; 11:190–196. [PubMed: 24412976]

Mendelson A, Frenette PS. Hematopoietic stem cell niche maintenance during homeostasis and regeneration. Nature medicine. 2014; 20:833–846.

Mendez-Ferrer S, Michurina TV, Ferraro F, Mazloom AR, Macarthur BD, Lira SA, Scadden DT, Ma'ayan A, Enikolopov GN, Frenette PS. Mesenchymal and haematopoietic stem cells form a unique bone marrow niche. Nature. 2010; 466:829–834. [PubMed: 20703299]

Mizoguchi T, Pinho S, Ahmed J, Kunisaki Y, Hanoun M, Mendelson A, Ono N, Kronenberg HM, Frenette PS. Osterix marks distinct waves of primitive and definitive stromal progenitors during bone marrow development. Developmental cell. 2014; 29:340–349. [PubMed: 24823377]

Moore KA, Lemischka IR. Stem cells and their niches. Science. 2006; 311:1880–1885. [PubMed: 16574858]

Morrison SJ, Scadden DT. The bone marrow niche for haematopoietic stem cells. Nature. 2014; 505:327–334. [PubMed: 24429631]

Novick D, Kim S, Kaplanski G, Dinarello CA. Interleukin-18, more than a Th1 cytokine. Seminars in immunology. 2013; 25:439–448. [PubMed: 24275602]

Okamura H, Tsutsi H, Komatsu T, Yutsudo M, Hakura A, Tanimoto T, Torigoe K, Okura T, Nukada Y, Hattori K, et al. Cloning of a new cytokine that induces IFN-gamma production by T cells. Nature. 1995; 378:88–91. [PubMed: 7477296]

Paic F, Igwe JC, Nori R, Kronenberg MS, Franceschetti T, Harrington P, Kuo L, Shin DG, Rowe DW, Harris SE, et al. Identification of differentially expressed genes between osteoblasts and osteocytes. Bone. 2009; 45:682–692. [PubMed: 19539797]

Patel AP, Tirosh I, Trombetta JJ, Shalek AK, Gillespie SM, Wakimoto H, Cahill DP, Nahed BV, Curry WT, Martuza RL, et al. Single-cell RNA-seq highlights intratumoral heterogeneity in primary glioblastoma. Science. 2014; 344:1396–1401. [PubMed: 24925914]

Picelli S, Faridani OR, Bjorklund AK, Winberg G, Sagasser S, Sandberg R. Full- length RNA-seq from single cells using Smart-seq2. Nature protocols. 2014; 9:171–181. [PubMed: 24385147]

Pridans C, Holmes ML, Polli M, Wettenhall JM, Dakic A, Corcoran LM, Smyth GK, Nutt SL. Identification of Pax5 target genes in early B cell differentiation. Journal of immunology. 2008; 180:1719–1728.

Shalek AK, Satija R, Shuga J, Trombetta JJ, Gennert D, Lu D, Chen P, Gertner RS, Gaublomme JT, Yosef N, et al. Single-cell RNA-seq reveals dynamic paracrine control of cellular variation. Nature. 2014; 510:363–369. [PubMed: 24919153]

Shapiro E, Biezuner T, Linnarsson S. Single-cell sequencing-based technologies will revolutionize whole-organism science. Nature reviews Genetics. 2013; 14:618–630.

Sugimura R, He XC, Venkatraman A, Arai F, Box A, Semerad C, Haug JS, Peng L, Zhong XB, Suda T, et al. Noncanonical Wnt signaling maintains hematopoietic stem cells in the niche. Cell. 2012; 150:351–365. [PubMed: 22817897]

Tang F, Barbacioru C, Wang Y, Nordman E, Lee C, Xu N, Wang X, Bodeau J, Tuch BB, Siddiqui A, et al. mRNA-Seq whole-transcriptome analysis of a single cell. Nat Methods. 2009; 6:377–382. [PubMed: 19349980]

Wang F, Flanagan J, Su N, Wang LC, Bui S, Nielson A, Wu X, Vo HT, Ma XJ, Luo Y. RNAscope: a novel in situ RNA analysis platform for formalin-fixed, paraffin-embedded tissues. The Journal of molecular diagnostics : JMD. 2012; 14:22–29. [PubMed: 22166544]

Xie T, Spradling AC. A niche maintaining germ line stem cells in the Drosophila ovary. Science. 2000; 290:328–330. [PubMed: 11030649]

Xie Y, Yin T, Wiegraebe W, He XC, Miller D, Stark D, Perko K, Alexander R, Schwartz J, Grindley JC, et al. Detection of functional haematopoietic stem cell niche using real-time imaging. Nature. 2009; 457:97–101. [PubMed: 19052548]

Zhang J, Niu C, Ye L, Huang H, He X, Tong WG, Ross J, Haug J, Johnson T, Feng JQ, et al. Identification of the haematopoietic stem cell niche and control of the niche size. Nature. 2003; 425:836–841. [PubMed: 14574412]

Zhu X, Hill RA, Dietrich D, Komitova M, Suzuki R, Nishiyama A. Age-dependent fate and lineage restriction of single NG2 cells. Development. 2011; 138:745–753. [PubMed: 21266410]

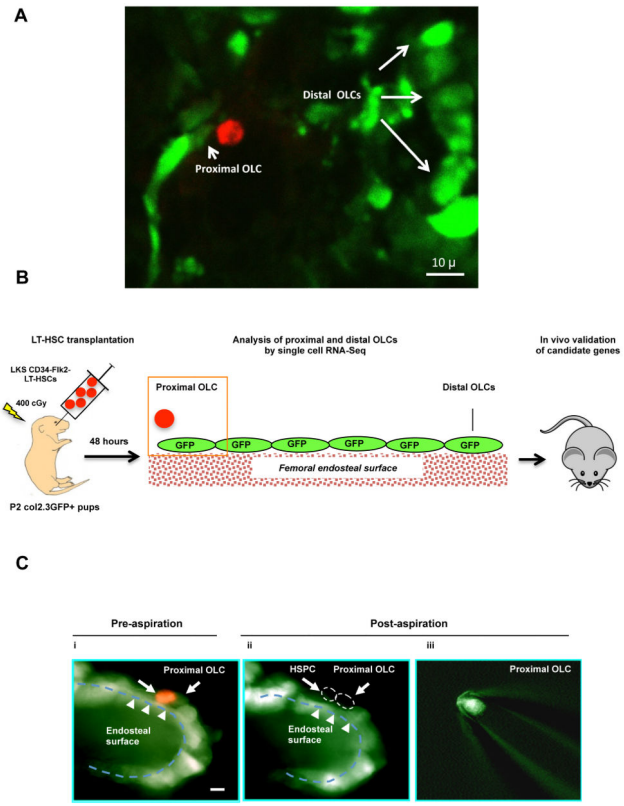

Figure 1. Proximity-based single cell analysis of the bone marrow niche

(A) Fluorescent microscopy image of femoral bone section from newborn col2.3GFP+ animal injected with DiI-labeled adult bone marrow LT-HSCs 48 hours after transplantation. Proximal OLC (circled) is defined as the nearest GFP+ cell within two cell diameters (red square) from HSPC (arrowhead). Distal cells are GFP+ cells located outside of this area at least five cell diameters away from transplanted HSPC (white arrows). Scale bar 10 microne. (B) Experimental workflow. (C) Example of micropipette aspiration of proximal OLC. Shown are overlaid single color (GFP and DiI) images before and after retrieval of proximal OLC (i) The proximal GFP^+ OLC (green) was identified based on proximity to the DiI-labeled HSPC (red). (ii, iii) Following in-situ enzymatic dissociation, HSPC was dislodged from its original location and proximal OLC was aspirated into a micropipette. Scale bar 10 microne.

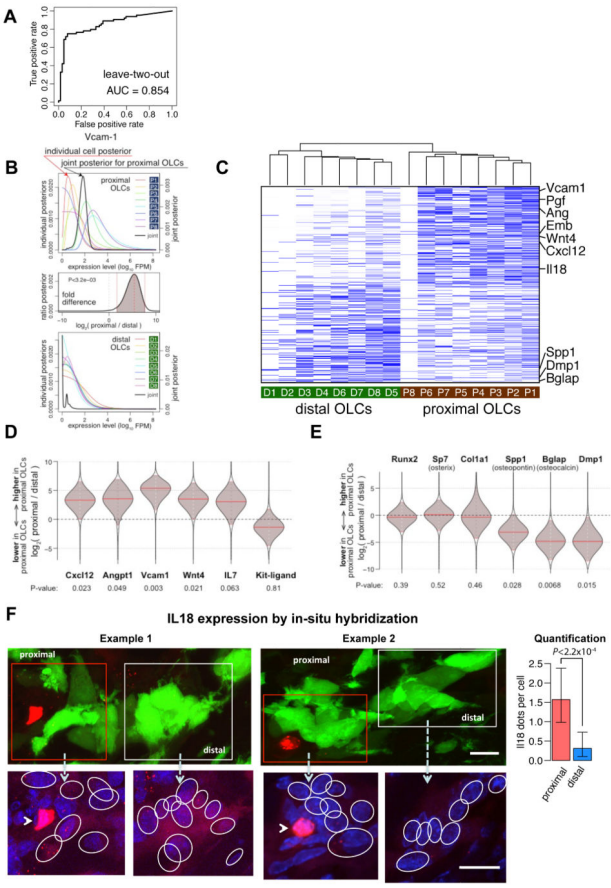

Figure 2. Transcriptional profiling of proximal and distal OLCs by single cell RNA-Seq

(A) An unbiased genome-wide classification of proximal and distal OLCs. The receiver-operator characteristic curve for the Support Vector Machine classification where all successive pairs of cells (one proximal and one distal) were classified based on the training data provided by other cells (P<0.005). (B) The use of SCDE to estimate the posterior distribution of expression levels based on the observations from each cell (colored lines, top and bottom panels). Analysis of the Vcam-1 gene is shown as an example. The joint posteriors (black lines) describe the overall estimation of likely expression levels within the proximal (top) and distal (bottom) OLCs, and are used to estimate the posterior of the expression fold difference (middle plot). The shaded area under the fold-difference posterior shows 95% confidence region.(C) Classification of individual OLCs based on the top 200 differentially expressed genes. Each row represents a gene, with the most likely gene expression levels indicated by color (blue – high, white – low/absent). (D,E) Expression analysis of known niche-derived HSPC regulators and OLC maturation genes. The violin plots show the posterior distribution of the expression fold-difference (y-axis, log2 scale) for each gene, with the shaded area marking the 95% confidence region (equivalent to the middle plot in B). The horizontal solid red lines show the most likely fold-change value. (F) Quantification of IL18 expression in neonatal post-transplant bone marrow niche by fluorescent in-situ hybridization (RNA Scope). Newborn col2.3GFP+ animals were transplanted with DiI-labeled long-term HSCs and sacrificed at 48 hours, as for cell harvesting experiments. Frozen sections of fixed undecalcified femoral bones were

hybridized with fluorescently-labeled IL18 probe. Maximal intensity projections over 12 microns are displayed. *Top panel:* Lower magnification images illustrating spatial definition of “proximal” (within two cell diameters from transplanted HSPC, arrowhead) and “distal” (greater than five cell diameters from transplanted HSPC) areas. *Bottom panel:* higher magnification images displaying DAPI stain (blue) and the RNA scope signal (red dots). The nuclei of GFP+ cells are circled. IL18 mRNA was quantified by comparing the intensity of the RNA scope signal (expressed as the average number of dots per cell) between GFP+ cells within proximal and distal areas, and the results are displayed in (E) ($p<2.2\times10^{-4}$, 95% confidence intervals are shown, based on the Poisson model of the dot occurrences per cell. P-value was estimated using Poisson rate ratio test).

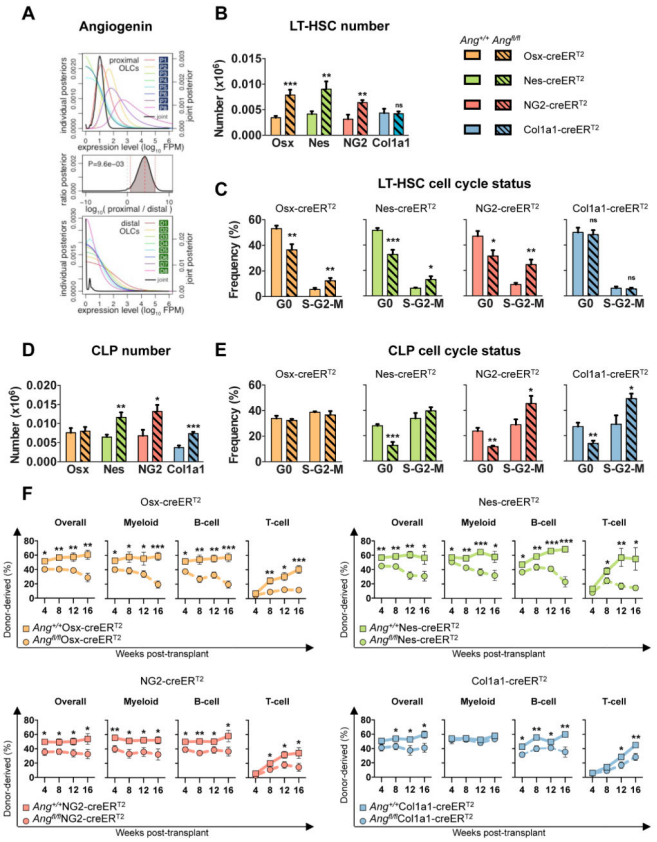

Figure 3. Conditional deletion of *Ang* from niche cell subsets leads to the loss of quiescence in LT-HSCs and CLPs

(A) Comparison of *Ang* expression in proximal and distal OLCs. (B) LT-HSC number per femur and (C) LT-HSC cell cycle status following conditional deletion of *Ang* from distinct niche cell subsets, as per the color-coded legend (n=4-10). Non-shaded graphs: control animals, shaded graphs: *Ang*-deleted animals. (D) CLP number per femur and (E) CLP cell cycle status following conditional deletion of *Ang* from distinct niche cell subsets (n=4-10). (F) Long-term reconstitution following competitive (1:1) transplantation of bone marrow from control animals (solid lines) and animals with conditional deletion of *Ang* (broken lines) into WT congenic recipients (n=8). **P*<0.05, ***P*<0.01, ****P*<0.001. Data are presented as mean+/− SEM.

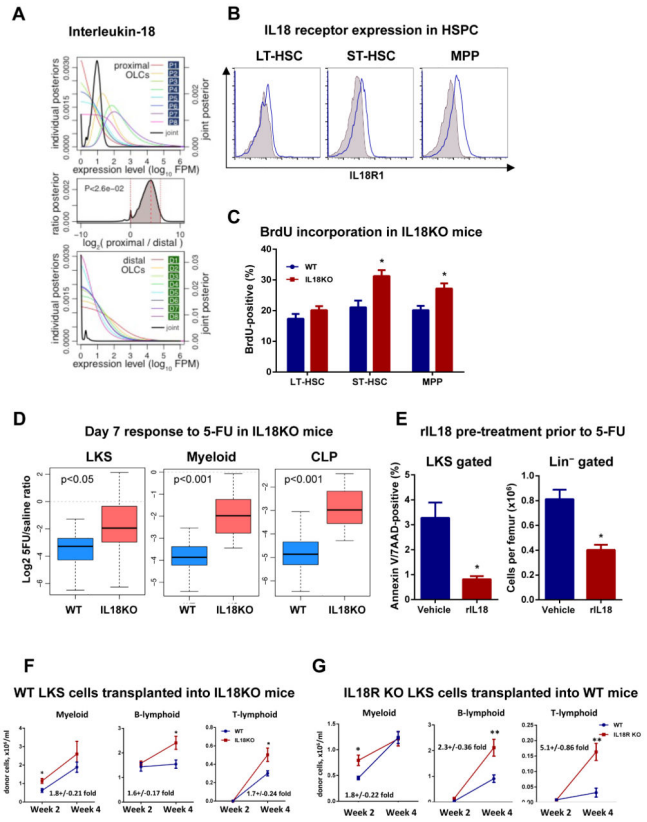

Figure 4. ***In vivo*** **analysis of IL18 function in HSPC regulation**

(A) Comparison of IL18 expression in proximal and distal OLC. (B) IL18 receptor expression in HSPC. Representative histograms are shown (n=3). A comparable cell population from IL18R KO mouse was used as a negative control (shaded histogram). (C) BrdU incorporation by HSPC in IL18KO mice (n=5). (D) Flow cytometric assessment of multi-lineage response to 5-FU in IL18KO mice. The statistical significance was assessed by ANOVA. Boxplots illustrating log ratios of cell numbers between 5- FU-treated and vehicle-treated animals in WT and IL18 groups are shown (n=7). (E) Enumeration of apoptotic LKS cells and lin-negative cells in WT animals pre-treated with rIL18 prior to 5-FU exposure (n=5). (F) Myeloid and lymphoid reconstitution in IL18KO mice following transplantation of (WT) LKS cells (n=7). (G) Myeloid and lymphoid reconstitution following transplantation of LKS cells from IL18R1KO or WT animals into WT hosts (n=8 per group). **P*<0.05, ***P*<0.01. Data are presented as mean+/− SEM.

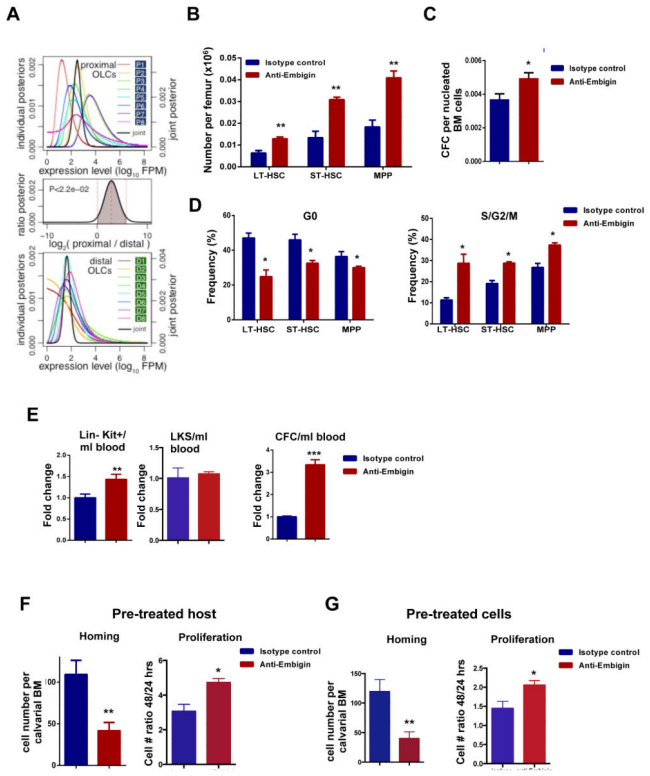

Figure 5. Identification of Embigin as a hematopoietic regulator

(A) Comparison of Embigin expression in proximal and distal OLC. (B) Quantification of primitive hematopoietic cells, (C) colony-forming cells and (D) cell cycle status following treatment with anti-Embigin or isotype control antibody (n=5). (E) The effect of anti-Embigin treatment on mobilization of $lin^{-}kit^{+}$ cells, $lin^{-}kit^{+}Sca1^{+}$ cells and colony-forming cells into peripheral blood (n=4). (F,G) Quantification of homing and proliferation by intra-vital microscopy following transplantation of WT LKS cells into anti-Embigin-treated host or anti-Embigin-treated LKS cells into WT host (n=4). Cell number per calvarial marrow at 24 hours and calculated proliferation rate based on assessment of cell number by repeat imaging at 48 hours comparing are shown. Green – transplanted GFP+ cells, blue – second harmonic generation (bone signal). * $p<0.05$, ** $p<0.01$. Data are presented as mean+/− SEM.

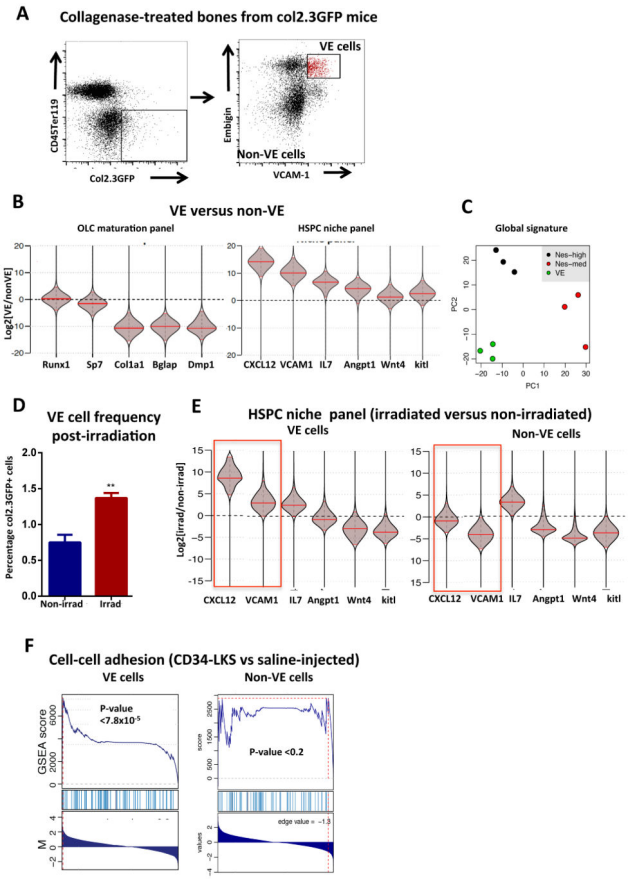

Figure 6. Isolation and characterization of VCAM^{+}Embigin^{high} subset of osteolineage cells (VE cells)

(A) Flow cytometric strategy for isolation of VE cells. (B) Expression of known niche factors and OLC maturation genes in VE cells from col2.3GFP mice (n=3). (C) Principal component analysis of transcriptomes from VE cells, nesitn-GFP^{high} and nestin-GFP^{low} cells (n=3). (D) Assessment of VE cell frequency after irradiation (n=4). (E) Changes in niche factor expression in VE cells following irradiation. (F) Results of GSEA analysis (cell-cell adhesion) in VE cells and non-VE cells from LT-HSC-versus saline-injected animals (n=3). Data are presented as mean+/− SEM.